From Master Slave Interferometry to Complex Master Slave Interferometry: theoretical work

Sylvain Rivet[*a,b], Adrian Bradu[b], Michael Maria[a,c], Thomas Feuchter[c], Lasse Leick[c] and Adrian Podoleanu[a]
[a]Applied Optics Group, School of Physical Sciences, University of Kent, Canterbury CT2 7NH, UK; [b]Université de Bretagne Occidentale, EA 938 Laboratoire d'Optique et de Magnétisme, Avenue Le Gorgeu, C.S. 93837, 29238 Brest Cedex 3, France; [c]NKT Photonics A/S, Blokken 84, DK-3460 Birkerod, Denmark

ABSTRACT

A general theoretical framework is described to obtain the advantages and the drawbacks of two novel Fourier Domain Optical Coherence Tomography (OCT) methods denoted as Master/Slave Interferometry (MSI) and its extension denoted as Complex Master/Slave Interferometry (CMSI). Instead of linearizing the digital data representing the channeled spectrum before a Fourier transform can be applied to it (as in OCT standard methods), channeled spectrum is decomposed on the basis of local oscillations. This replaces the need for linearization, generally time consuming, before any calculation of the depth profile in the range of interest. In this model two functions, *g* and *h*, are introduced. The function g describes the modulation chirp of the channeled spectrum signal due to nonlinearities in the decoding process from wavenumber to time. The function h describes the dispersion in the interferometer. The utilization of these two functions brings two major improvements to previous implementations of the MSI method. The paper details the steps to obtain the functions *g* and *h*, and represents the CMSI in a matrix formulation that enables to implement easily this method in LabVIEW by using parallel programming with multi-cores.

Keywords: Optical coherence tomography; Medical optics instrumentation; Multiple imaging; Ophthalmic optics and devices.

1. INTRODUCTION

Spectrometer based Optical Coherence Tomography (Sp-OCT) and Swept Source based Optical Coherence Tomography (SS-OCT) [1,2] are technologies based on analyzing the spectrum of the interference signal produced between optical signal from an object under investigation and a local optical reference signal. OCT can produce in real time a cross section image of the object, *i.e.* a two dimensional image. The prior art executes spectral analysis using a Fourier transform (FT) of the spectrum of the interference $I^{chirped}$, which necessitates to remove the chirp of the channeled spectra before any FT can be applied to it. This chirp has two origins: 1) the nonlinear dependence of the pixel position in the spectrometer versus the optical frequency or the non-linear frequency sweeping of the swept-source, 2) the unbalanced dispersion in the interferometer arms that also affects the regularity of maxima and minima in the readout channeled spectrum. Nevertheless numerical methods to correct chirping before FT are time consuming.

Master-Slave Interferometry (MSI) [3] and Complex Master-Slave Interferometry (CMSI) [4] are new approaches to Fourier domain OCT that do not require the step of linearization. They are tolerant to any chirping of the spectrum and can proceed to calculation of the depth information profile (A-scan) on the depth of interest. In certain circumstances, as detailed below, this is more time efficient than using resampling followed by a FT. The MSI and CMSI methods proceed in two stages. In a first stage (Master), a mirror is used as an object and experimental channeled spectra (CS_{exp}) are measured. In a second stage (Slave), the object replaces the mirror and the channeled spectrum is compared with local oscillations determined during the Master stage. These local oscillations characterize the system in terms of its chirp, due to nonlinearities and dispersion. Each local oscillation associated to a required depth is mixed with the channeled spectrum (obtained using the sample) and the result is in fact the value of the A-Scan at these required depths. For MSI, the local oscillations are the CS_{exp} measured at different values of the optical path difference (OPD) in the interferometer, and the comparison operation is a correlation product [3] or several simplified dot product procedures for faster implementation of correlation [5,6]. For CMSI, the local oscillations are synthesized functions evaluated from a reduced set of acquired experimental channeled spectra. These functions incorporate the non-linearity of the spectrometer (or the swept source) and the unbalanced dispersion in the interferometer. The comparison operation for CMSI is only a simple dot product.

In this proceeding, the theoretical framework on MSI and CMSI is presented.

2. PROPERTIES OF MSI

Let us consider a non-uniform distribution of wave number $\tilde{k}$ along the pixels of the line array detector when using a spectrometer, or along time when using a tunable laser (swept source). The relationship between the optical wave number k and $\tilde{k}$ is given by the function $g(\tilde{k}) = k$.

For each depth of interest, z, the MSI method consists in mixing the channeled spectrum $I^{chirped}$ collected when the sample is placed in the object arm (Slave stage) with the channeled spectrum CS_{exp} collected at the Master stage for an OPD = $2z$, when the mirror is used as an object. The comparison operation is then the maximum of the correlation product between $I^{chirped}$ and CS_{exp} as follows:

$$MSI(z) = \underset{T}{Max}\left[\int_{-\infty}^{+\infty} I^{chirped}\left(\tilde{k}\right) CS_{\exp}\left(\tilde{k}+T, z\right) d\tilde{k}\right]. \tag{1}$$

The correlation product is affected by the random phase shift φ_{rand} induced by the fluctuations of the OPD between the step of acquiring the channeled spectra CS_{exp} to be used as local oscillations and the step of measuring the channeled spectrum $I^{chirped}$ associated to the object. Without random variation, MSI can be written as the dot product between $I^{chirped}$ and CS_{exp}

$$MSI(z) = \int_{-\infty}^{+\infty} I^{chirped}\left(\tilde{k}\right) CS_{\exp}\left(\tilde{k}, z\right) d\tilde{k}\ , \tag{2}$$

that represents the correlation product for argument zero. For a single-layer sample whose reflection is R at an axial distance z_0, the MSI signal can be expressed according to the Parseval theorem, as follows

$$MSI(z) = \Re e\left[R(z_0)\delta(z-z_0) \otimes FT\left\{\left|A(k)\right|^2 \frac{dG(k)}{dk}\right\}\right], \tag{3}$$

where $A(k)$ represents the interference contrast, $\otimes$ is the convolution product, δ is the Dirac function and G is defined as the inverse function of g, $G(g) \equiv 1$.

The MSI method is independent of the amount of dispersion left uncompensated in the interferometer, meaning that the axial resolution is not affected. This property has already been demonstrated in [7]. Additionally, as the decoding non-linearity described by dG/dk is the same at all OPD values, the axial resolution is also independent on z but it is not optimal, as Eq. (3) involves the square of A than simply A (if the chirp is removed before the FT). For instance if A has a Gaussian shape, the axial resolution is $\sqrt{2}$ poorer than the axial resolution obtained with the FT method without any unbalanced dispersion and nonlinearities. Equation (3) also shows that combination of phase in the complex R with the random phase impedes the recovery of the complex R.

3. PROPERTIES OF CMSI

3.1 Synthesized local oscillations

The experimental channeled spectra CS_{exp} measured during the Master stage depend on the non-linearity of the spectrometer or the swept-source $g\left(\tilde{k}\right) = k$, and the function $h\left(\tilde{k}\right)$ related to the unbalanced dispersion of the interferometer according to the following expression:

$$CS_{\exp}\left(\tilde{k}, z\right) = I_{DC}\left(g\left(\tilde{k}\right)\right) + A\left(g\left(\tilde{k}\right)\right) e^{i\left(g\left(\tilde{k}\right)2z + h\left(\tilde{k}\right)\right) + \varphi_{rand}(\pi)} + CC\ , \tag{4}$$

where I_{DC} follows the shape of the power spectrum of the optical source and CC means complex conjugate.

A simple way to extract the functions *g* and *h* consists in following three steps as described below.

1st step: extraction of the phase

Figure 1 shows how to extract the phase of the experimental channeled spectra CS_{exp} measured during the Master stage. The procedure is based on a Fourier transform calculation, a high-pass filter to remove the DC component and the conjugate term , and the argument calculation of complex values.

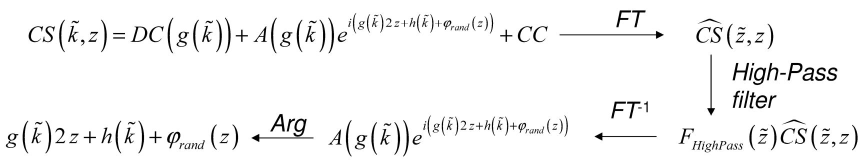

Figure 1. Diagram explaining the process of extracting the phase of a real channeled spectrum related to a mirror as sample. Arg means argument calculation.

The measured phase ϕ related to CS_{exp} is then equal to

$$\phi\left(\tilde{k},z\right)=g\left(\tilde{k}\right)2z+h\left(\tilde{k}\right)+\varphi_{rand}\left(z\right). \tag{5}$$

2nd step: random phase removed

The phase is then subtracted from the value of the phase measured at the centre of the spectrum $\tilde{k}_0$. This procedure removes the random phase induced by the fluctuations of the OPD during the Master stage:

$$\phi\left(\tilde{k},z\right)-\phi\left(\tilde{k}_0,z\right)=\left(g\left(\tilde{k}\right)-g\left(\tilde{k}_0\right)\right)2z+\left(h\left(\tilde{k}\right)-h\left(\tilde{k}_0\right)\right). \tag{6}$$

3rd step: linear regression

A linear regression applied to the phase experimental phase for each value of $\tilde{k}$, according to *z*, permits to extract the functions $g(\tilde{k})$ and $h(\tilde{k})$. As a further simplification, we consider that $g(\tilde{k})$ and $h(\tilde{k})$ are equal to zero at the center of the spectrum. A minimum of n = 2 CS_{exp} are needed to extract the functions $g(\tilde{k})$ and $h(\tilde{k})$, while in practice, for enhanced accuracy, we normally acquire n = 5 CS_{exp}. The linear regression can be expressed in matrix format as:

$$\begin{bmatrix} g\left(\tilde{k}\right)-g\left(\tilde{k}_0\right) \\ h\left(\tilde{k}\right)-h\left(\tilde{k}_0\right) \end{bmatrix}=P^{+}\begin{bmatrix} \phi\left(\tilde{k},z_1\right)-\phi\left(\tilde{k}_0,z_1\right) \\ \vdots \\ \phi\left(\tilde{k},z_n\right)-\phi\left(\tilde{k}_0,z_n\right) \end{bmatrix}, \tag{7}$$

where P^+ is the pseudo-inverse matrix of P defined by:

$$P=\begin{bmatrix} 2z_1 & 1 \\ \vdots & \vdots \\ 2z_n & 1 \end{bmatrix}, \tag{8}$$

z_1, .., z_n being the different positions of the mirror used at the Master stage for which CS_{exp} are collected.

The local oscillations (masks) are built to obtain the same point spread function as that delivered by the standard method (where the chirp is removed by resampling, followed by application of a TF). The masks are complex and sensitive to the phase of *R* . They are generated for each depth of interest *z*:

$$M_{built}(\tilde{k},z)=\frac{dg\left(\tilde{k}\right)}{d\tilde{k}}Exp\left[i\left(\frac{2\pi}{c}g\left(\tilde{k}\right)2z+h\left(\tilde{k}\right)\right)\right]. \tag{9}$$

3.2 Comparison operation between $I^{chirped}$ and M_{built}

CMSI involves a similar definition to the MSI except that the CS_{exp} used as local oscillations are replaced by a complex function with the adjustable parameter z. CMSI is valid for an object set outside OPD = 0, *i.e.* CMSI signal is defined similarly to Eq. (2) by the following integral:

$$CMSI(z) = \int_{-\infty}^{+\infty} I^{chirped}(\tilde{k}) M^*_{built}(\tilde{k}, z) d\tilde{k} . \quad (10)$$

As with the MSI, CMSI has been described above by continuous variables, however practical implementations involve digital processing. In this case one point of the A-Scan in depth is equivalent to a dot product between a mask vector and the acquired spectrum, $I^{chirped}$. An A-scan from z_1 to z_Z can be written as a product between a matrix containing M_{built} for different depths and the vector (or array) $I^{chirped}$ as shown below:

$$\left[Ascan(z_1),\ldots,Ascan(z_Z)\right] = \begin{bmatrix} \left[M^*_{built}(\tilde{k}_1, z_1)\cdots M^*_{built}(\tilde{k}_K, z_1)\right] \\ \vdots \\ \left[M^*_{built}(\tilde{k}_1, z_Z)\cdots M^*_{built}(\tilde{k}_K, z_Z)\right] \end{bmatrix} \bullet \begin{bmatrix} I^{chirped}(\tilde{k}_1) \\ \vdots \\ I^{chirped}(\tilde{k}_K) \end{bmatrix}, \quad (11)$$

where $\tilde{k}_1,\ldots,\tilde{k}_K$ correspond to the sampling along the pixels in the spectrometer line camera or along the time slots within the sweeping time for a swept source and where z_1, .., z_Z correspond to the different OPDs required by the user independently from the number of CS_{exp} acquired at the Master stage.

Due to the matrix expression of CMSI and the reduction of operations according to the depth of interest, CMSI method can provide real-time cross-sectional images in LabVIEW [8] thanks to high performance toolboxes that take advantage of the multicore design of modern processors.

3.3 Properties of CMSI

For a single-layer sample whose reflection is R at depth z_0, CMSI can be expressed as follows

$$CMSI(z) = R(z_0)\delta(z - z_0) \otimes FT\{A(k)\} . \quad (12)$$

Depth information profile is extracted and expressed as a convolution product between a complex reflectivity function and the ideal PSF of the system, which leads to a constant axial resolution in depth irrespective of the non-linearity of the decoder and irrespective of the amount of the unbalanced dispersion in the interferometer.

The drawbacks of the previous implementations of MSI are overcome by CMSI: (i) the depth points of the A-scan are now determined by a sampling parameter z, independent of the OPD values used to acquire the CS_{exp} at the Master stage, (ii) CMSI operation returns a complex signal, hence phase of R is conserved. (iii) The axial resolution is related to FT[A], as for a perfect interferometer.

3.4 Different expressions of the local oscillations

In order to decrease the amplitude of secondary lobes in Fourier domain and improve the quality of the image in depth, a window function W is usually applied with the Fourier transformation of the channeled spectra. With CMSI, the same strategy can be used, and the synthesized local oscillations become:

$$M_{W,built}(\tilde{k}, z) = W(\tilde{k}) \frac{dg(\tilde{k})}{d\tilde{k}} Exp\left[i\left(\frac{2\pi}{c} g(\tilde{k}) 2z + h(\tilde{k})\right)\right]. \quad (13)$$

Another functionality is to have the possibility of removing the DC component of the channeled spectrum $I^{chirped}$. In this case, the synthesized local oscillations can be written as:

$$M_{F,built}(\tilde{k}, z) = FT^{-1}\left\{F_{HighPass}(\tilde{z}) FT\left\{M_{built}(\tilde{k}, z)\right\}\right\}, \quad (14)$$

where $F_{HighPass}$ is a high pass filter to remove the DC component.

4. CONCLUSION

The theoretical expression for the operation of CMSI is identical to the Fourier transform of channeled spectra for a perfect interferometer (no dispersion) and perfect decoder, such as either a spectrometer linear in wavenumber or a linearly tunable swept source, however with the difference that the CMSI delivers a complex signal without random phase shift. This allows CMSI to eliminate the process of window integration practiced in the MSI, integration that has lead to worsening the axial resolution. Having access to the phase, CMSI method can be further explored to measure the phase of signal acquired from the object. Lastly CMSI method can provide real-time cross-sectional images in LabVIEW thanks to high performance toolboxes that take advantage of the multicore design of processors.

ACKNOWLEDGEMENTS

S. Rivet acknowledges the Marie-Curie Intra-European Fellowship for Career Development, No. 625509. M. Maria, T. Feuchter, L. Leick and A. Podoleanu acknowledge the UBAPHODESA Marie Curie European Industrial Doctorate 607627. A. Bradu and A. Podoleanu acknowledge the support of ERC (http://erc.europa.eu) COGATIMABIO 249889. and REBOT EPSRC EPN0192291.A. Podoleanu is also supported by the ERC (http://erc.europa.eu) AdaSmartRes 754695, NIHR Biomedical Research Centre at Moorfields Eye Hospital NHS Foundation Trust - UCL Institute of Ophthalmology and by the Royal Society Wolfson Research Merit Award.

*sylvain.rivet@univ-brest.fr

REFERENCES

[1] J. Fujimoto, "Optical coherence tomography for ultrahigh resolution in vivo imaging," Nat. Biotechnol. **21**, 1361-1367 (2003)

[2] D. Huang, E. A. Swanson, C. P. Lin, J. S. Schuman, W. G. Stinson, W Chang, M. R. Hee, T Flotte, K Gregory, C. A. Puliafito and J. G. Fujimoto, "Optical coherence tomography," Science **254**, 1178-1181 (1991).

[3] A. G. Podoleanu and A. Bradu, "Master-slave interferometry for parallel spectral domain interferometry sensing and versatile 3D optical coherence tomography," Opt. Express **21**(16), 19324–19338 (2013).

[4] S. Rivet, Michael Maria, Adrian Bradu, Thomas Feuchter, Lasse Leick and Adrian Podoleanu, « Complex Master Slave Interferometer, » Optics Express **24**(3), 2885-2904 (2016).

[5] A. Bradu and A. G. Podoleanu, "Imaging the eye fundus with real-time en-face spectral domain optical coherence tomography," Biomed. Opt. Express **5**(4), 1233–1249 (2014).

[6] J. Wang, A. Bradu, G. Dobre, and A. Podoleanu, "Full-field swept source master slave optical coherence tomography," IEEE Photonics Journal **7**(4), 1943-0655 (2015).

[7] A. Bradu, M. Maria, and A. Podoleanu, "Demonstration of tolerance to dispersion of master/slave interferometry," Opt. Express **23**(11), 14148-14161 (2015).

[8] A. Bradu, S. Rivet, A. Podoleanu, "Master/slave interferometry – the ideal tool for coherence revival swept source optical coherence tomography," Biomed. Opt. Express **7**(7), 2453-2468 (2016).